



Research.Publish.Connect.



Proceedings

Proceedings of the 10th International Conference on Computer Vision Theory and Applications - (Volume 3)

March 11-14, 2015, in Berlin, Germany



Editors: José Braz ¹ ; Sebastiano Battiato ² and Francisco Imai ³

Affiliations: ¹ Escola Superior de Tecnologia de Setúbal, Portugal ; ² University of Catania, Italy ; ³ Canon U.S.A. Inc., Innovation Center, United States

ISBN: 978-989-758-091-8

Conference Link: <http://www.visapp.visigrapp.org/>

Foreword: This book contains the proceedings of the 10th edition of the International Conference on Computer Vision Theory and Applications (VISAPP) which was organized and sponsored by the Institute for Systems and Technologies of Information, Control and Communication (INSTICC), in cooperation with ACM SIGGRAPH and technically co-sponsored by IEEE Computer Society, IEEE VGTC and IEEE Technical Committee on Multimedia Computing. Since its first edition in 2006, VISAPP has been bringing together researchers from all over the world to share new knowledge, insights, and experimental results in these areas. The conference focused on five different Computer Vision areas, from "Image Formation and Preprocessing" to "Image

and Video Analysis” including “Image and Video Understanding”, “Applications and Services” and “Motion, Tracking and Stereo Vision”. All tracks focus on real world applications and highlight the benefits of Computer Vision for industry and services, thus making a bridge between **(More)**

Volumes:

Vol. 1 - 978-989-758-089-5

Vol. 2 - 978-989-758-090-1

Vol. 3 - 978-989-758-091-8

Papers

Authors

Show papers

A Comprehensive Approach for Evaluation of Stereo Correspondence Solutions in Augmented Reality

P. 5 -
13

Bahar Pourazar and Oscar Meruvia-Pastor

DOI:10.5220/00052725

Blind Watermarking using QIM and the Quantized SVD Domain based on the q-Logarithm Function

P. 14 -
25

Ta Minh Thanh and Keisuke Tanaka

DOI:10.5220/00052919

Handwritten Text Verification on Mobile Devices

P. 26 -
33

Nilson Donizete Guerin Júnior , Flávio de Barros Vidal and Bruno Macchiavello

DOI:10.5220/00053552

A Multi-resolution Approach for Combining Visual Information using Nuclei Segmentation and Classification in Histopathological Images

P. 37 -
46

Harshita Sharma , Norman Zerbe , Daniel Heim , Stephan Wienert , Hans-Michael Behrens , Olaf Hellwich and Peter Hufnagl

DOI:10.5220/00052479

Extraction of Homogeneous Regions in Historical Document Images

P. 47 -
54

Maroua Mehri , Pierre Héroux , Nabil Sliti , Petra Gomez-Krämer , Najoua Essoukri Ben Amara and Rémy Mullot

DOI:10.5220/00052655

Depth Camera to Improve Segmenting People in Indoor Environments - Real Time RGB-Depth Video Segmentation

P. 55 -
62

Arnaud Boucher , Olivier Martinot and Nicole Vincent

DOI:10.5220/00052697

Data Acquisition in Cast Iron Foundries by Image Analysis

P. 63 -
70

Bernd Dreier , Florian Blas and Alexander Kostgeld

DOI:10.5220/00052816

PCB Recognition using Local Features for Recycling Purposes

P. 71 -
78

Christopher Pramerdorfer and Martin Kampel

DOI:10.5220/00052892

-
- Real-time Detection and Recognition of Machine-Readable Zones with Mobile Devices** P. 79 - 87
Andreas Hartl , Clemens Arth and Dieter Schmalstieg **DOI:10.5220/00052947**
-
- A Posterization Strategy for the Registration of [123I]FP-CIT SPECT Brain Images** P. 88 - 92
Diego Salas-Gonzalez , Elmar W. Lang , Juan M. Gorriz and Javier Ramírez **DOI:10.5220/00052960**
-
- Selective Encryption of Medical Images** P. 93 - 99
Aissa Belmeguenai , Lakhdar Grouche and Rafik Djemili **DOI:10.5220/00053012**
-
- Semi-automatic Analysis of Huge Digital Nautical Charts of Coastal Aerial Images** P. 100 - 107
Matthias Vahl , Uwe von Lukas , Bodo Urban and Arjan Kuijper **DOI:10.5220/00053015**
-
- Securing Iris Images with a Robust Watermarking Algorithm based on Discrete Cosine Transform** P. 108 - 114
Mohammed A. M. Abdullah , S. S. Dlay and W. L. Woo **DOI:10.5220/00053057**
-
- The “Everywhere Switch” using a Projector and Camera** P. 115 - 122
Akira Nozaki and Katsuto Nakajima **DOI:10.5220/00053076**
-
- A Simple Real-Time Eye Tracking and Calibration Approach for Autostereoscopic 3D Displays** P. 123 - 129
Christian Bailer , José Henriques , Norbert Schmitz and Didier Stricker **DOI:10.5220/00053091**
-
- On the Assessment of Segmentation Methods for Images of Mosaics** P. 130 - 137
Gianfranco Fenu , Nikita Jain , Eric Medvet , Felice Andrea Pellegrino and Myriam Pilutti Namer **DOI:10.5220/00053101**
-
- Computing Corpus Callosum as Biomarker for Degenerative Disorders** P. 138 - 149
Thomas Kovac , Sammy Rogmans and Frank Van Reeth **DOI:10.5220/00053102**
-
- Robust Watermarking Algorithm for 3D Multiresolution Meshes** P. 150 - 157
Ikbel Sayahi , Akram Elkefi , Mohamed Koubaa and Chokri Ben Amar **DOI:10.5220/00053164**
-
- On Line Video Watermarking - A New Robust Approach of Video Watermarking based on Dynamic Multi-sprites Generation** P. 158 - 165
Ines Bayoudh , Saoussen Ben Jabra and Ezzeddine Zagrouba **DOI:10.5220/00053168**
-
- Automatic Generation of Suitable DWT Sub-band - An Application to Brain MRI Classification** P. 166 - 170

Image-based Ear Biometric Smartphone App for Patient Identification in Field Settings

P. 171 -
179

Sarah Adel Bargal , Alexander Welles , Cliff R. Chan ,
Samuel Howes , Stan Sclaroff , Elizabeth Ragan ,
Courtney Johnson and Christopher Gill

DOI:10.5220/00053422

Copyright Protection for 3D Printing by Embedding Information Inside Real Fabricated Objects

P. 180 -
185

Masahiro Suzuki , Piyarat Silapasuphakornwong ,
Kazutake Uehira , Hiroshi Unno and Youichi Takashima

DOI:10.5220/00053424

Automatic Identification of Mycobacterium tuberculosis in Ziehl-Neelsen Stained Sputum Smear Microscopy Images using a Two-stage Classifier

P. 186 -
191

Lucas de Assis Soares , Klaus Fabian Coco , Evandro Ottoni
Teatini Salles and Saulo Bortolon

DOI:10.5220/00053452

Towards a 3D Pipeline for Monitoring and Tracking People in an Indoor Scenario using Multiple RGBD Sensors

P. 192 -
200

Konstantinos Amplianitis , Michele Adduci and Ralf Reulke

DOI:10.5220/00053566

Watermark Embedding and Extraction Scheme Design by Two-stage Optimization for Illegal Replication Detection of Two-dimensional Barcodes

P. 201 -
208

Satoshi Ono , Kentaro Nakai , Takeru Maehara and Ryo Ikeda

DOI:10.5220/00053581

An Augmented Environment for Command and Control Systems

P. 209 -
214

Alessandro Zocco , Lucio T. De Paolis , Lorenzo Greco and
Cosimo L. Manes

DOI:10.5220/00053589

Visualization 3D Reconstruction - Volume Rendering of Mucus into Paranasal Sinuses

P. 215 -
220

Rodrigo Freitas Lima and Mauricio Marengoni

DOI:10.5220/00053591

A Technique for Computerised Brushwork Analysis

P. 221 -
226

Dmitry Murashov , Alexey Berezin and Ekaterina Ivanova

DOI:10.5220/00053623

Salient Parts based Multi-people Tracking

P. 231 -
240

Zhi Zhou , Yue Wang and Eam Khwang Teoh

DOI:10.5220/00052622

Semantic Segmentation and Model Fitting for Triangulated Surfaces using Random Jumps and Graph Cuts

P. 241 -
250

Tilman Wekel and Olaf Hellwich

DOI:10.5220/00052651

- Fast Adaptive Frame Preprocessing for 3D Reconstruction** P. 260 - 267
Fabio Bellavia , Marco Fanfani and Carlo Colombo **DOI:10.5220/00052727**
-
- TextTrail - A Robust Text Tracking Algorithm In Wild Environments** P. 268 - 276
Myriam Robert-Seidowsky , Jonathan Fabrizio and Séverine Dubuisson **DOI:10.5220/00052920**
-
- A Rolling Shutter Compliant Method for Localisation and Reconstruction** P. 277 - 284
Gaspard Duchamp , Omar Ait-Aider , Eric Royer and Jean-Marc Lavest **DOI:10.5220/00052955**
-
- SPHERA - A Unifying Structure from Motion Framework for Central Projection Cameras** P. 285 - 293
Christiano Couto Gava and Didier Stricker **DOI:10.5220/00053017**
-
- TVL1 Shape Approximation from Scattered 3D Data** P. 294 - 304
Eugen Funk , Laurence S. Dooley and Anko Boerner **DOI:10.5220/00053018**
-
- Optimal Surface Normal from Affine Transformation** P. 305 - 316
Barath Daniel , Jozsef Molnar and Levente Hajder **DOI:10.5220/00053037**
-
- A Convex Framework for High Resolution 3D Reconstruction** P. 317 - 324
Min Li , Changyu Diao , Song Lv and Dongming Lu **DOI:10.5220/00053065**
-
- Real-time Accurate Pedestrian Detection and Tracking in Challenging Surveillance Videos** P. 325 - 334
Kristof Van Beeck and Toon Goedemé **DOI:10.5220/00053087**
-
- Bio-inspired Model for Motion Estimation using an Address-event Representation** P. 335 - 346
Luma Issa Abdul-Kreem and Heiko Neumann **DOI:10.5220/00053115**
-
- Improving the Egomotion Estimation by Correcting the Calibration Bias** P. 347 - 356
Ivan Krešo and Siniša Šegvić **DOI:10.5220/00053161**
-
- Evaluation of 3D Analysis Error Caused by SVP Approximation of Fisheye Lens** P. 357 - 368
Nobuyuki Kita **DOI:10.5220/00053174**
-
- Edge based Foreground Background Estimation with Interior/Exterior Classification** P. 369 - 376
Gianni Allebosch , David Van Hamme , Francis Deboeverie , Peter Veelaert and Wilfried Philips **DOI:10.5220/00053580**
-

How to Choose the Best Embedded Processing Platform for on-Board UAV Image Processing ?

Dries Hulens , Jon Verbeke and Toon Goedemé

P. 377 -
386

DOI:10.5220/00053594

Improved Confidence Measures for Variational Optical Flow

Maren Brumm , Jan Marek Marcinczak and Rolf-Rainer Grigat

P. 389 -
394

DOI:10.5220/00051672

Temporal Selection of Images for a Fast Algorithm for Depth-map Extraction in Multi-baseline Configurations

Dimitri Bulatov

P. 395 -
402

DOI:10.5220/00052395

Discrete Optimal View Path Planning

Sebastian Haner and Anders Heyden

P. 411 -
419

DOI:10.5220/00052521

Towards Human Pose Semantic Synthesis in 3D based on Query Keywords

Mo'taz Al-Hami and Rolf Lakaemper

P. 420 -
427

DOI:10.5220/00052587

BarvEye - Bifocal Active Gaze Control for Autonomous Driving

Ernst Dieter Dickmanns

P. 428 -
436

DOI:10.5220/00052585

An Image-based Ensemble Kalman Filter for Motion Estimation

Yann Lepoittevin , Isabelle Herlin and Dominique Béréziat

P. 437 -
445

DOI:10.5220/00052598

A Self-adaptive Likelihood Function for Tracking with Particle Filter

Séverine Dubuisson , Myriam Robert-Seidowsky and Jonathan Fabrizio

P. 446 -
453

DOI:10.5220/00052600

Prev 1 2 Next

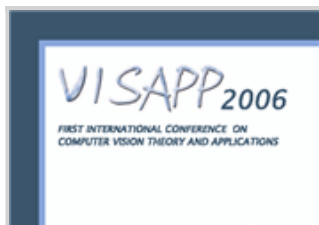
DETAILS OF RELATED PROCEEDINGS

Other proceedings of same conference

Proceedings of the First
International Conference on
Computer Vision Theory and
Applications

Proceedings of the Second
International Conference on
Computer Vision Theory and
Applications

Proceedings of the Second
International Conference on
Computer Vision Theory and
Applications



SCITEPRESS - SCIENCE AND TECHNOLOGY PUBLICATIONS, LDA.

RESOURCES

Proceedings

Papers

Authors

Ontology

CONTACTS

Science and Technology

Publications, Lda

Avenida de S. Francisco

Xavier, Lote 7 Cv. C,

2900-616 Setúbal,

Portugal.

Phone: +351 265 520 185

Fax: +351 265 520 186

Email: info@scitepress.org

EXTERNAL LINKS

PRIMORIS

INSTICC

SCITEVENTS

CROSSREF

PROCEEDINGS SUBMITTED FOR INDEXATION BY:

Thomson Reuters

dblp

Ei Compendex

SCOPUS

Semantic Scholar

Blind Watermarking using QIM and the Quantized SVD Domain based on the q -Logarithm Function

Ta Minh Thanh^{1,2} and Keisuke Tanaka^{1,3}

¹Dept. of Computer Science, Tokyo Institute of Technology, Tokyo, 152-8552, Japan

²Dept. of Network Security, Le Quy Don Technical University, 236 Hoang Quoc Viet, Cau Giay, Ha Noi, Vietnam

³CREST, JST., Tokyo, Japan

Keywords: q -Logarithm SVD (q -SVD), Image Watermarking, Quantization Index Modulation (QIM).

Abstract: We propose new image blind watermarking by using both the quantization index modulation (QIM) technique and the quantized singular value decomposition (SVD) domain based on the q -logarithm function. In order to reduce the distortion of the embedded image, we employ the q -logarithm transform on the Y component of the original image after performing the SVD domain. We call this domain the q -SVD domain. In our proposed method, the tradeoff of robustness and quality can be controlled by a predefined quantization coefficient Q of QIM and a parameter q of the q -SVD domain. Several experiments are conducted to show the robustness of our proposed method against processing attacks and geometric attacks.

1 INTRODUCTION

1.1 Background

Due to the advance of computer and network techniques, e-business of digital contents has become the most popular market for various types of digital contents such as picture, audio, movie, and so on. However, since network applications have become very popular, everyone can easily copy, alter, or even steal digital content via network. Therefore, the protection of digital content in e-business has become one of the most important issue.

Digital watermarking is a promising technique in order to protect the digital content by embedding the watermark directly into digital content. The embedded watermark can be extracted later for authentication, copyright protection, and traitor detection (Shih, 2008; Yeung, 1998; Nikolaidis and Pitas, 2003; Bao and Ma, 2005; Liu and Tan, 2002).

In general, the invisibility, robustness, and capacity of the watermark are important requirements for the proposed watermarking. The watermark should not make visible changes on digital content in order to remain the quality of the original image. Additionally, the watermark must be robust against the image attacks/distortions applied to the embedded content. Finally, the watermark must be easily extracted

to prove ownership and to detect the traitor.

There are two types of the digital watermarking methods, the spatial domain watermarking and the transform domain watermarking.

In the spatial domain watermarking, the watermark information is embedded directly into the components of the original content, for example, an RGB component by altering its values (Yeung, 1998). The spatial watermarking domain has advantages such as low complexity and simple implementation. However, the spatial domain watermarking methods are not robust against image processing attacks, and geometric attacks.

The transform domain watermarking methods embed the watermark by modifying the magnitude of coefficients in transform domain such as discrete Fourier transformation (DFT), discrete cosine transform (DCT), discrete wavelet transform (DWT), and singular value decomposition (SVD) (Nikolaidis and Pitas, 2003; Bao and Ma, 2005; Liu and Tan, 2002). Also, there have been a lot of proposals of watermarking methods that use the mixed domain. For instance, the combination of DCT and SVD (Liu and Liu, 2008; Lu et al., 2007; Yavuz and Telatar, 2006), that of SVD and DWT (Cao et al., 2009; Yavuz and Telatar, 2007; Zhang and Li, 2009), that of DWT and DCT (Deb et al., 2012; Feng et al., 2010; Bei et al., 2011) are employed to embed the watermark into the digital con-

tent. Embedding on transform domain seems more robust but rather complicated to compute because of its high computation cost. Additionally, the previous methods only focused on the robustness of the watermark by sacrificing the quality of the embedded content.

In particular, the SVD-based technique is used to efficiently extract algebraic features from an image. Based on the feature of SVD transform, the stable SVD matrices feature of image can be easily obtained. Therefore, when the image is degraded by several image processing attacks, its singular values (SVs) do not change significantly (Liu and Tan, 2002; Lai, 2011; Zhou and Chen, 2004). This feature is normally used to embed the user's information into the image with less degradation.

As shown in the papers (Liu and Tan, 2002; Lai, 2011; Zhou and Chen, 2004; Bhatnagar and Raman, 2009), SVD-based watermarking algorithms were proposed. In order to achieve the robustness, Liu and Tan (Liu and Tan, 2002) presented a watermark method which embeds the watermark into the singular values of matrix S . Three matrices U_w , S , and V_w are saved as the secret key. These matrices are required in the watermark extraction. In order to extend the method of (Liu and Tan, 2002), Lai *et al.*: (Lai, 2011) demonstrated a watermarking technique using SVD and a tiny genetic algorithm to achieve the robustness of the watermark information. Unfortunately, both algorithms of (Liu and Tan, 2002) and (Lai, 2011) are fundamentally flawed as mentioned in (Loukhaoukha, 2013). This bug of these algorithms causes false positive detection even if the attacker uses a different embedded watermark or the secret key. In the method of Chandra *et al.*: (Chandra, 2002), not only the original image is required but also the original watermark during the watermark extraction process. Hence, their method is not suitable for real applications. Bao (Bao and Ma, 2005) utilized the quantization parameter for enhancing the quality of the watermarked image. In the extraction process, the quantization parameter is required as the private key. However, the original image must to be transformed to the wavelet and SVD domain. It requires high computation cost.

As mentioned above, the previous SVD-based watermarking techniques mainly focused on the robustness of embedding methods but did not the quality of the watermarked images.

1.2 Our Contributions

We consider that it is very important to improve the quality of the embedded content, while maintaining the robustness of watermarking methods.

We extend the original SVD domain to the q -logarithm SVD domain in order to improve the quality of image and to retain the robustness of watermarking method. In particular, we make the following contributions in this paper:

(1) Inspired by the motivation of (Tsallis, 1998), we present the novel frequency domain, called q -logarithm SVD domain (q -SVD), for the image watermarking that is not proposed before. – See Section 2.

(2) We investigate the efficiency of the combinations of both parameters Q and q for our method. We find out the appropriate values for Q and q suitable for watermark embedding. By these combinations, the tradeoff of the robustness and the quality can be controlled by a predefined quantization coefficient Q of QIM and a parameter q of the q -SVD transform. – See Section 4.2.

(3) Various simulation experiments are conducted to demonstrate the performance of our proposed method. Experimental results show that the proposed method has stronger robustness against most common attacks such as the JPEG compression, cropping, swirl, and so on. – See Section 4.3.

Therefore, by using our method, we simultaneously improve the quality of embedded image also achieve the robustness of the watermark.

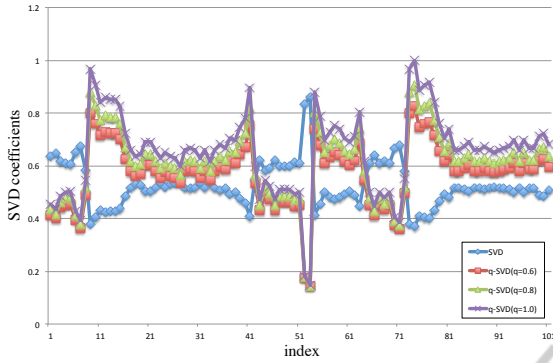
1.3 Roadmap

The rest of this paper is organized as follows. The proposed q -SVD domain is described in Section 2 and we will explain why the q -SVD domain is suitable for our watermarking method. Section 3 describes our proposed watermarking method using QIM on the q -SVD domain. Our simulation results are shown in Section 4. Section 5 concludes our paper.

2 QUANTIZED SVD DOMAIN BASED ON q -LOGARITHM FUNCTION

2.1 q -Logarithm and q -Exponential Function

q -logarithm and its inverse, q -exponential, are the concept of non-extensive statistics which is intro-


 Figure 1: The comparison of SVD and q -SVD.

duced by Tsallis (Tsallis, 1998), a theory of non-extensive statistics. The q -logarithm function is defined as follows:

$$\log_q(x) = \frac{x^{1-q} - 1}{1-q} \quad (1)$$

and its converse, q -exponential is defined as:

$$\exp_q(x) = (1 + (1-q)x)^{\frac{1}{1-q}}; \quad (2)$$

where the parameter q is a real number that is predetermined and x is also a real number. In our work, x can be a pixel of image or a coefficient of the frequency domain.

Inspired by the theory of non-extensive statistics, we propose q -SVD domain to provide a novel frequency domain, which is very flexible by randomly choosing q parameter to control the quality of image after inverse transform. We employ the feature of q -logarithm and q -exponential in Eq. (1) and Eq. (2) to construct q -SVD for image processing.

2.2 Proposed q -SVD Domain

Suppose that the image I with size $N \times N$ is divided into non-overlapping blocks. Each block is a matrix, called A , with size 8×8 .

In general, the real matrix A can be decomposed into three matrices $SVD(A) = USV^T$, where U and V are orthogonal matrices, such that $UU^T = E$, $VV^T = E$ and $S = \text{diag}(l_1; l_2; \dots)$. Here, the singular values $l_1; l_2; \dots$ of matrices A are sorted decreasingly, and E is the unit matrix.

There are the following advantages when using SVD in digital image processing:

- (1) It is not necessary to fix the size of the matrix A beforehand. Its size is $x \times x$ or $x \times y$ for some $x; y$. Therefore, we can choose the size of A suitable for that of the watermark image.

- (2) SVs of a digital image are less affected under the general image processing such as blurring, noise addition, slight rotation. Therefore the quality of the watermarked image can be kept after embedding.

Inspired by the theory of non-extensive statistics (Tsallis, 1998), we propose the q -SVD domain, which is very flexible by arbitrary choosing the parameter q to control the quality of image. We employ the feature of q -logarithm and q -exponential (Tsallis, 1998) to construct the q -SVD for image processing.

Suppose an image I is given. First, I is transformed into q -logarithm as follows:

$$I_q(i; j) = \log_q fI(i; j)g = \frac{fI(i; j)g^{1-q} - 1}{1-q}; \quad (3)$$

where $I(i; j)$ and $I_q(i; j)$ represent the pixel (coefficient) at coordinate $(i; j)$ of the spatial domain and the q -logarithm domain, respectively. The matrix A_q from I_q can be transformed to q -SVD using the original SVD. The q -SVD domain of I is defined as $SVD(A_q)$. We call the resulting U , S , and V^T as q -SVD domain.

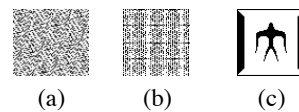
After performing the SVD, we adjust the values of U , S , or V^T to control the quality of image. In order to reconstruct the image I^q , we apply SVD again to obtain I_q^q based on the adjusted values of U , S , and V^T . Finally, we perform the q -exponential function:

$$I^q(i; j) = \exp_q(I_q^q(i; j)) = (1 + (1-q)I_q^q(i; j))^{\frac{1}{1-q}}; \quad (4)$$

Since the values of image pixels are slightly changed after applying the q -logarithm transform, the low-frequency of q -SVD domain is considered to be very suitable for the image watermarking method. Therefore, the watermarking based on q -SVD can be expected not only to improve the quality of the embedded image, but also to keep the robustness of the watermark information.

2.3 Advantage of the q -SVD

In the previous watermarking researches, the watermark is directly added into the coefficient of the frequency domain. Therefore, it causes the distortion in quality of the embedded digital content. In our proposed frequency domain, q -SVD, the coefficient of the classical frequency domain is then quantized by q -logarithm transformation. The modification of


 Figure 2: Permuted watermark by the Torus permutation after p times, where a) $p=20$, b) $p=60$, c) $p=96$.

$$S_w(u, v) = \begin{cases} S(u, v)/Q \times Q + \text{sgn}(S(u, v)) \times 3Q/4 & \text{if } w_i = 1, \\ S(u, v)/Q \times Q + \text{sgn}(S(u, v)) \times Q/4 & \text{if } w_i = 0, \end{cases}$$

where $S(u; v)$ and $S_w(u; v)$ are the SVs of the block S in the q -SVD domain at the coordinate $(u; v)$ of the original image and the watermarked image, respectively. sgn function equals to “+” if $S(u; v) > 0$, “-” if $S(u; v) < 0$. $\lfloor \cdot \rfloor$ denotes the floor function. Q denotes the embedding strength chosen to maintain the quality of embedded image.

Step 4. Perform the SVD again to make the watermarked matrix A and to obtain Y_q^0 .

Step 5. Apply the q -exponential function for Y_q^0 to obtain Y^0 . Include Cb, Cr component with Y^0 and transform YCbCr space to RGB color for reconstructing the watermarked image I^0 .

According to the embedding process, we embed the watermark W^0 into the q -SVD domain of the Y component. Thus, we can control the quality of the embedded image based on two parameters: the parameter q for q -SVD domain, and the parameter Q for watermark strength. Therefore, our proposed method is more flexible than conventional methods using the SVD domain.

3.3 Watermark Extraction Algorithm

The extraction is performed without using the original image and those steps are described in following. Basic steps involved in the watermarking extraction, shown in Figure 4, are given as follows:

Step 1. Convert the RGB image I^k to YCbCr color space. Transform Y^k component using the q -logarithm transformation to obtain Y_q^k . Divide Y_q^k into the non-overlapping blocks. The size of each block is the size used in the embedding process.

Step 2. Perform SVD on each block A^k to obtain the SVs of each block.

Step 3. Extract the binary sequence of the watermark from matrices S^k based on the following rule:

$$w_i^k = \begin{cases} 1 & \text{if } S^k(u; v) \geq \lfloor S^k(u; v) \rfloor \geq Q/2 \text{ and } \text{sgn}(S^k(u; v)) \geq Q/2; \\ 0 & \text{if } S^k(u; v) \geq \lfloor S^k(u; v) \rfloor < Q/2 \text{ and } \text{sgn}(S^k(u; v)) \geq Q/2; \end{cases} \quad (6)$$

Step 4. From $f w_i^k g$, we can obtain the permuted watermark W^k . Permute W^k with P - p times using Torus permutation, we can obtain the extracted watermark W^{00} .

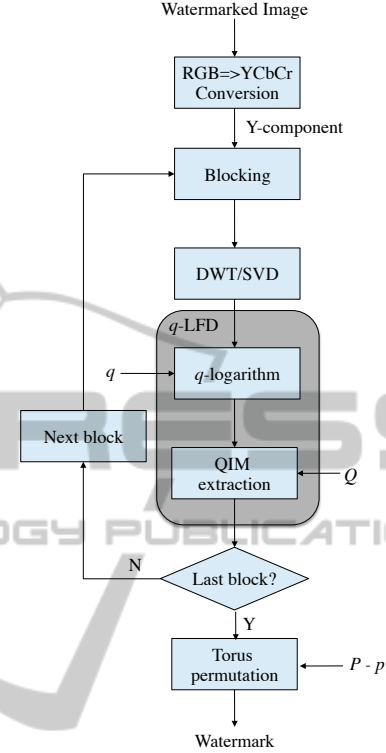


Figure 4: Extraction based on q -SVD.

4 SIMULATION RESULTS

4.1 Test Images and Evaluational Measures

To assess the performance of the proposed algorithm, we conduct four colors images of the well known SIDBA (Standard Image Data-BASE) database¹. All test images have size 512 \times 512 pixels. The watermark image is a binary image with size 64 \times 64 shown in Figure 2(c).

In order to evaluate the quality of watermarked images, we employ PSNR (Peak Signal to Noise Ratio) criterion (Thanh et al., 2014). The PSNR of N \times N pixels of image $I(i; j)$ and $I'(i; j)$ is calculated by:

¹www.vision.kuee.kyoto-u.ac.jp/IUE/IMAGE_DATA BASE/STD_IMAGES/

Table 1: PSNR[dB], NC values using q and Q .

| Q | q | 0.2 | 0.4 | 0.6 | 0.8 | 1.2 | 1.4 | 1.6 | 1.8 | 2.0 |
|------|------|----------|----------|----------|----------|----------|----------|----------|----------|----------|
| 0.30 | PSNR | 38.4593 | 40.3052 | 41.9444 | 43.2561 | 45.5018 | 46.3084 | 47.0307 | 47.5226 | 48.1225 |
| | NC | 0.971029 | 0.964782 | 0.956682 | 0.941818 | 0.918022 | 0.89495 | 0.885542 | 0.862428 | 0.85067 |
| 0.35 | PSNR | 36.8905 | 38.7757 | 40.4758 | 41.9163 | 44.2819 | 45.3985 | 46.1682 | 46.8607 | 47.2839 |
| | NC | 0.977358 | 0.969377 | 0.963476 | 0.941196 | 0.938796 | 0.910206 | 0.883629 | 0.876834 | 0.860438 |
| 0.40 | PSNR | 35.4971 | 37.4385 | 39.1805 | 40.6326 | 43.2493 | 44.1945 | 45.214 | 46.0372 | 46.6467 |
| | NC | 0.980723 | 0.974017 | 0.968718 | 0.94935 | 0.945882 | 0.92807 | 0.896696 | 0.880235 | 0.85553 |
| 0.45 | PSNR | 34.1959 | 36.205 | 37.9389 | 39.5019 | 42.0997 | 43.2704 | 44.178 | 45.13 | 45.8973 |
| | NC | 0.984111 | 0.978375 | 0.969048 | 0.962175 | 0.943057 | 0.930975 | 0.903418 | 0.89034 | 0.871261 |
| 0.50 | PSNR | 33.0911 | 35.0678 | 36.8297 | 38.4515 | 41.1907 | 42.3449 | 43.3211 | 44.2749 | 45.1378 |
| | NC | 0.984111 | 0.982753 | 0.975685 | 0.975763 | 0.94511 | 0.939008 | 0.917181 | 0.891637 | 0.877551 |
| 0.55 | PSNR | 32.0909 | 34.0549 | 35.8289 | 37.4512 | 40.2472 | 41.4019 | 42.568 | 43.3395 | 44.4058 |
| | NC | 0.985472 | 0.985131 | 0.979374 | 0.970037 | 0.945847 | 0.943396 | 0.93117 | 0.900313 | 0.887457 |
| 0.60 | PSNR | 31.1681 | 33.1005 | 34.9007 | 36.5316 | 39.3755 | 40.5954 | 41.6975 | 42.716 | 43.5228 |
| | NC | 0.98855 | 0.985131 | 0.981737 | 0.973684 | 0.945569 | 0.940174 | 0.928848 | 0.911775 | 0.887944 |
| 0.75 | PSNR | 30.2909 | 32.2614 | 34.0562 | 35.711 | 38.5476 | 39.9008 | 41.0083 | 42.0944 | 42.8494 |
| | NC | 0.987179 | 0.985813 | 0.985131 | 0.97435 | 0.949017 | 0.945729 | 0.92867 | 0.913636 | 0.904137 |

$$PSNR = 20 \log \frac{255}{MSE} \quad [\text{dB}] \quad (7)$$

$$MSE = \frac{1}{N \delta N} \sum_{i=0}^{N-1} \sum_{j=0}^{N-1} f(i; j) \delta f(i; j)^2$$

(MSE : Mean Square Error):

To judge the robustness, we use the normalized correlation (NC) value between the original watermark W and the extracted watermark W^m (Thanh et al., 2014). The value of NC is calculated by:

$$NC = \frac{\sum_{i=0}^{63} \sum_{j=0}^{63} [W(i; j) \delta W^m(i; j)]}{\sqrt{\sum_{i=0}^{63} \sum_{j=0}^{63} [W(i; j)]^2}} \quad (8)$$

where $W(i; j)$ and $W^m(i; j)$ are the original watermark bit and the extracted bit at the position $(i; j)$.

In our experiments, we calculate the PSNR value for each embedded image and the NC value for each watermark extracted from the embedded images and the attacked images. In general, if the PSNR value is over 37dB, the quality of the embedded image is considered to be close to the original image. When the NC value is close to 1, it means that the watermarking method is robust against the attacks.

4.2 Quality Evaluation and Optimization of Parameters Q and q

In our method, by increasing the parameter Q of QIM, we can achieve the robustness of the watermarking method. However, the visible distortion of the embedded image is more conspicuous. Fortunately, by

increasing the parameter q of the q -SVD, we can improve the quality of the embedded image with keeping the robustness of the watermark.

In order to optimize the values of the parameters q and Q , we estimate the parameters q and Q for obtaining the visual quality of the embedded image and the robustness of the watermark information. To compare the average PSNR and the average NC values obtained from the embedded images based on $fQ; qg$, the watermark strength Q and the parameter q of the q -SVD are increased with uniform steps until we can achieve the minimum acceptable PSNR and NC value. Those are 37 dB for the PSNR and 0.9 for the NC, respectively.

The experimental results of the color image, Lena, are given in Table 1. According to the results shown in Table 1, it can be observed that we can control the visual quality of the watermarked image and the robustness of the watermark information based on the parameter q of q -SVD domain and the embedding strength parameter Q . When q is larger, the PSNR value is larger. It means that the visual quality of the embedded image is better if q increases. When Q is larger, the NC value is close to 1. It means that the robustness of watermark is better if Q increases. Therefore, to achieve high quality of the embedded image and the robustness of watermark, we can choose the appropriate parameters q and Q for the watermarking method.

In order to find the appropriate values for the parameters Q and q , we set the upper bound and the lower bound values of these parameters Q and q . In our experiments, we cannot arbitrarily increase the value of Q and decrease the value of q because the quality of the embedded image may become worse in the case of PSNR < 37 dB. On the other hand, we also

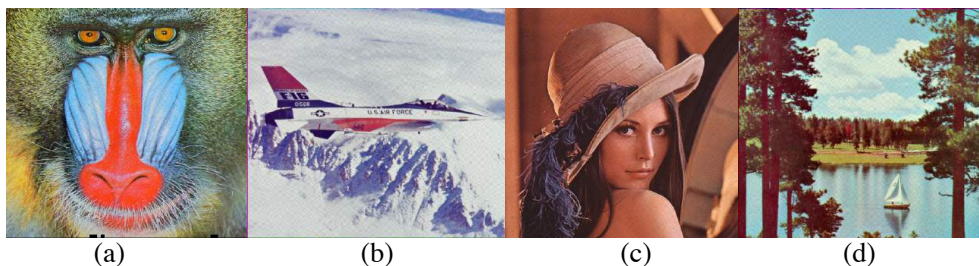


Figure 5: The watermarked color images ($q = 1.2; Q = 0.40$). (a) Baboon, PSNR=33.39, (b) F16, PSNR=35.90, (c) Lena, PSNR=43.67, and (d) Scene, PSNR=39.25.

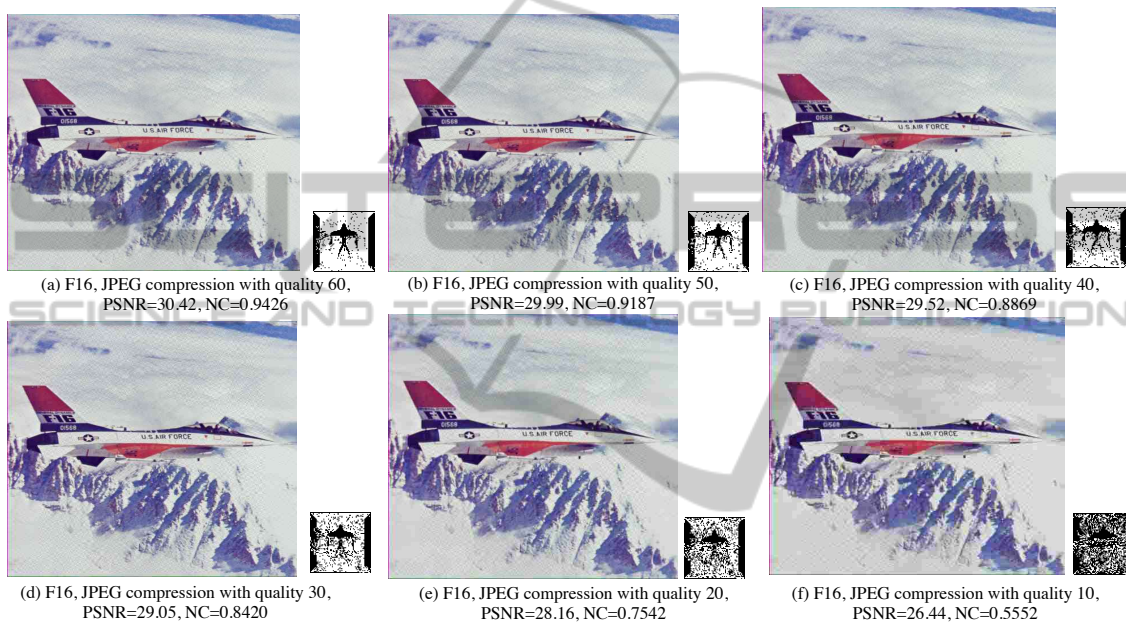


Figure 6: Watermarks extracted from embedded image F16 after JPEG compression with quality factors 60, 50, 40, 30, 20, and 10, respectively, when $q = 1.2; Q = 0.40$.

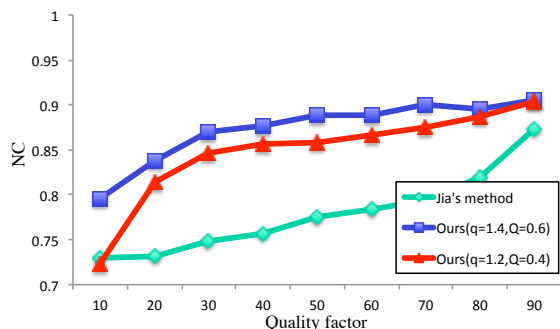


Figure 7: JPEG compression attack.

cannot decrease the value of Q and increase the value of q to obtain the better quality of the embedded images because this may decrease the robustness of the watermark in the case of $NC < 0.9$. By considering the upper bound and lower bound values, the appropriate values for the parameters Q and q are in the gray region shown in Table 1.

4.3 Simulation Results and Comparison

Without loss of generality, we choose $fq = 1.2; Q = 0.40g$ and $fq = 1.4; Q = 0.60g$ to simulate the experimental images. We embed the watermark into the original image and try to extract the watermark from the suspected image under intentional and unintentional attacks.

In order to evaluate the robustness of our proposed method, we compare our results with that of the method of Jia (Jia, 2014). In the case of Jia's method, to be fair, we implement his method employing the grayscale watermark instead of the color watermark.

4.3.1 Robustness Against JPEG Compression

Robust against JPEG compression is a basic requirement for the image watermarking. Therefore, we test our proposed method against JPEG compression with various quality factors. The simulation results

Table 2: PSNR[dB], NC values under JPEG compression with QF ($q = 1.2; Q = 0.40$)/($q = 1.4; Q = 0.60$).

| Image | Quality factor | No attack | 90 | 80 | 70 | 60 | 50 |
|--------|----------------|-------------|-------------|-------------|-------------|-------------|-------------|
| Lena | PSNR | 43.67/41.08 | 37.04/36.35 | 32.75/32.47 | 31.92/31.70 | 31.37/31.17 | 30.96/30.78 |
| | NC | 0.952/0.951 | 0.877/0.881 | 0.808/0.830 | 0.752/0.786 | 0.706/0.744 | 0.667/0.696 |
| F16 | PSNR | 35.90/32.38 | 33.85/31.30 | 31.44/29.80 | 30.92/29.44 | 30.41/29.08 | 29.99/28.81 |
| | NC | 0.996/0.994 | 0.989/0.986 | 0.982/0.978 | 0.963/0.974 | 0.943/0.961 | 0.919/0.946 |
| Baboon | PSNR | 33.39/32.83 | 29.22/29.00 | 25.76/25.66 | 25.12/25.03 | 24.62/24.54 | 24.24/24.17 |
| | NC | 0.961/0.966 | 0.906/0.911 | 0.814/0.823 | 0.761/0.795 | 0.725/0.766 | 0.686/0.725 |
| Scene | PSNR | 39.25/35.73 | 31.82/30.86 | 28.52/28.00 | 28.09/27.55 | 27.77/27.34 | 27.44/27.17 |
| | NC | 0.981/0.980 | 0.889/0.887 | 0.811/0.830 | 0.662/0.762 | 0.595/0.673 | 0.576/0.600 |

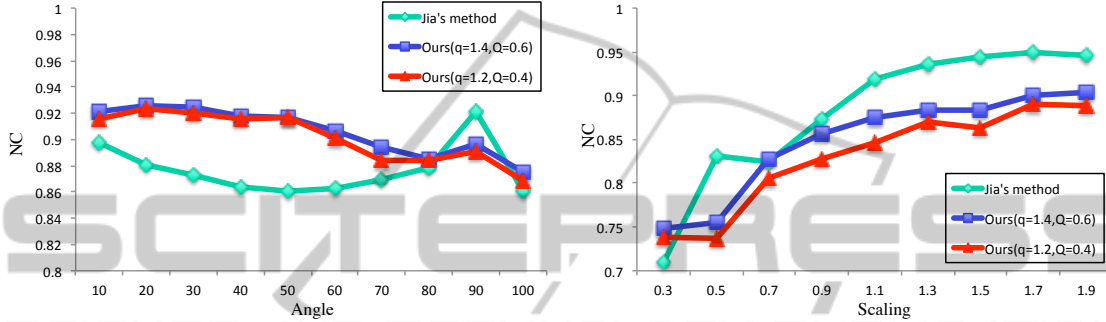


Figure 8: Geometric attack.

of the color images, Baboon, F16, Lena, and Scene, are given in Figure 5 and Table 2. Table 2 shows the NC values of the extracted watermarks and the PSNR values of the watermarked images after attacking by JPEG compression with different quality factors (QF). In the JPEG compression, the QF for the compression process is ranged from 1 to 100, which denotes the predetermined image quality of the JPEG compression. When QF is larger, lower compression ratio of the JPEG image is obtained and better visual quality of the JPEG image is retained.

According to Table 2, we find that even if under high compression ratios, high NC values can be obtained. It means that our proposed method is robust against the JPEG compression attack. The image watermarking needs to be robust against, at least, JPEG compression to ensure for image transmission via network. Note that, image is always compressed to JPEG image with quality factor equals to 75%80 before transmission. Figure 6 illustrates the watermark extracted from the embedded image F16 after the JPEG compression with low quality factors 60, 50, 40, 30, 20, and 10. It is clear that the extracted watermarks can be easily recognized by human eyes. Additionally, Figure 7 shows that our methods achieve better performance compared to Jia's method (Jia, 2014). Therefore, according to the results of Table 2 and Figure 7, our proposed method is useful under the JPEG compression and image transmission via network.

Comparing the results of Table 2, we find that when we use $f_q = 1.4; Q = 0.60g$ instead of $f_q =$

$1.2; Q = 0.40g$, the visual quality of watermarked images are remained, and the robustness of watermark is improved. Normally, when the parameter Q is increased, the quality of the embedded image is degraded. However, by using the larger q of the q -SVD domain, the quality of the embedded image is improved.

4.3.2 Robustness Against Geometric and Processing Attacks

In our experiments, the embedded images are subject to the following attacks.

Firstly, the geometric attacks are considered as the first challenge because they destroy the synchronization in the embedded image. The embedded images are scaled with different scaling factors (scaling attack). They are also rotated by several angles (rotation attack). The scaling factors with ranging from 0.3 to 1.9 and the rotation angles with ranging from 10° to 100° are employed in our tests. In order to obtain good extraction, the attacked image should be rescaled or re-rotated by an estimated scaling factor or an estimated rotation angle in the opposite direction. To be fair, the estimation algorithm in (Thanh et al., 2014) is performed. The results in Figure 8 shows that our methods are better than the method of Jia (Jia, 2014) in the rotation attacks. However, our methods in the scaling attacks are worse than the method in (Jia, 2014).

Secondly, noise addition attack is common distur-

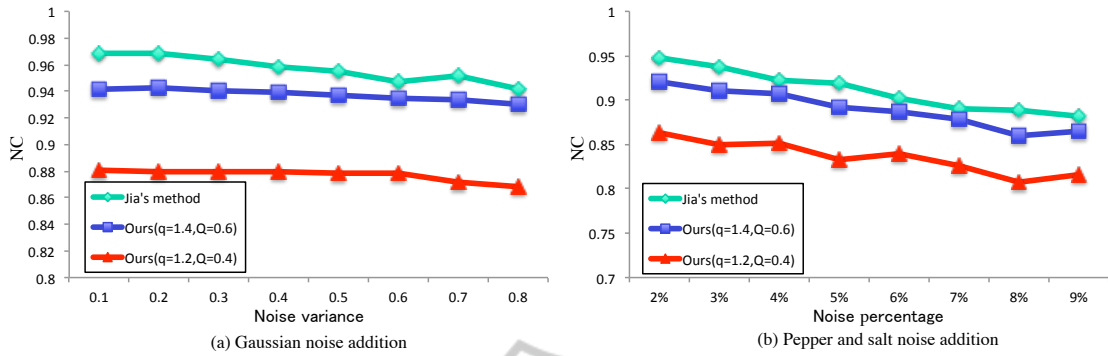


Figure 9: Noise addition attack.

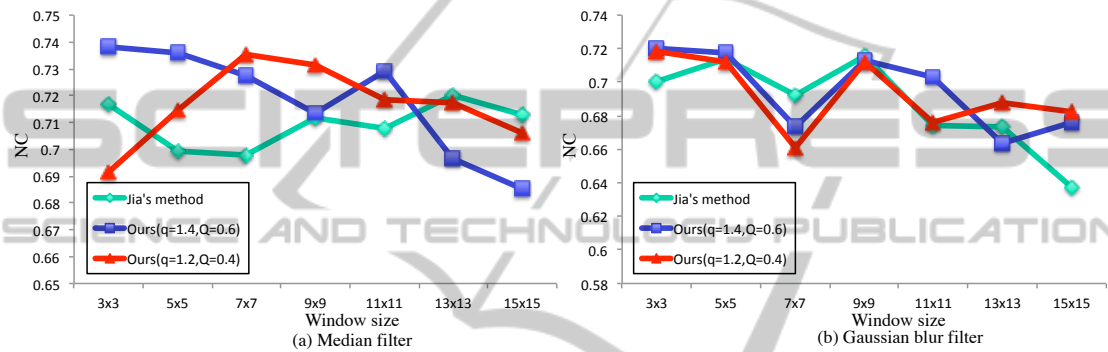


Figure 10: Filtering attack.

tion in which the noise is added to the embedded image. There are two types of noise, Gaussian white noise and ‘pepper and salt’ noise, which are normally added into the embedded images. For the purpose of our experiments, Gaussian white noise of zero mean and variance ranging from 0.1 to 0.9, and ‘pepper and salt’ noise with percentage ranging from 2% to 9% are added into the embedded image. As shown in Figure 9, our methods are not as robust against the Gaussian noise and ‘pepper and salt’ noise as the method of Jia (Jia, 2014). However, as we can see the watermark image in Figure 6 with $NC > 0.8$, the watermark image has still good quality. Hence, our methods can be acceptable under the noise addition attacks since the NC values of the extracted watermark are over 0.8.

Thirdly, the filtering attack is also tested in our experiments. There are two kinds of the filtering attacks, median filtering and Gaussian blur filtering, are used and adopted with window sizes are 3 δ 3; 5 δ 5; 7 δ 7; 9 δ 9; 11 δ 11; 13 δ 13; 15 δ 15. As in Figure 10, we can assert our proposed methods are better than the method in (Jia, 2014) under strong filtering attacks.

Fourthly, we present the shearing attack on the embedded images. In our experiment, the shearing percentages in x axes with ranging from 10% to 90%

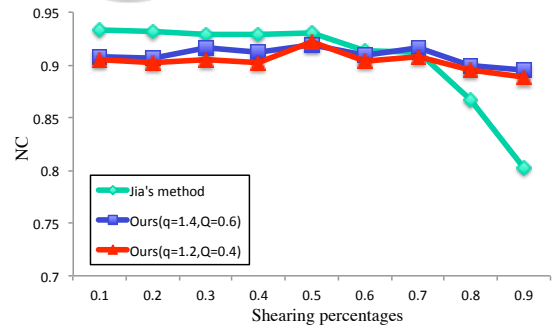


Figure 11: Shearing attack.

are applied. For re-shearing the attacked images, to be fair, we also use the method in (Thanh et al., 2014). After re-shearing, the watermark images are extracted from the the re-sheared images. As shown in Figure 11, our methods achieve better performance compared to (Jia, 2014) when the shearing percentages become higher.

For showing the robustness of our proposed method, we pick up several extracted watermark image of Lena image compared to Jia’s method. It can be seen from Figure 12, the robustness of watermark in the proposed method is better than (Jia, 2014).

In order to show the robustness of our proposed




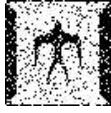












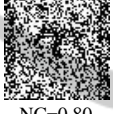


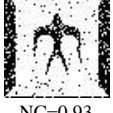

| Attack type | Jia's method | Ours ($q=1.4, Q=0.6$) | Ours ($q=1.2, Q=0.4$) |
|------------------------------|--|--|---|
| Rotation 40° |  NC=0.86 |  NC=0.92 |  NC=0.91 |
| Scaling 1.5 |  NC=0.94 |  NC=0.88 |  NC=0.86 |
| 'Pepper and salt' noise 9% |  NC=0.88 |  NC=0.86 |  NC=0.85 |
| JPEG QF=50 |  NC=0.77 |  NC=0.89 |  NC=0.86 |
| Median filter 7x7 |  NC=0.69 |  NC=0.73 |  NC=0.71 |
| Shearing 90% |  NC=0.84 |  NC=0.80 |  NC=0.87 |
| Gaussian noise, variance=0.8 |  NC=0.95 |  NC=0.93 |  NC=0.94 |

Figure 12: Comparison of extracted watermarks in terms of visual perception, NC values for Lena image.

method against common image processing attacks, we apply several attacks to the embedded Lena image such as tampered attacks by text "TA MINH", quarter of cropping, center cropping with radius of cycle equals to 100, 2/3 of cropping, grayscale and swirl attack. Here, we extract the watermark image from those attacked images and calculate the NC values. The results are illustrated in Figure 13. We can also easily recognize the watermark by human eyes.

5 CONCLUSION

A robust image watermarking based on the q -SVD domain using QIM technique have been proposed in this paper. As far as we know, it is the first scheme for watermarking. The watermark is embedded into the low-frequency of q -SVD domain in order to achieve

the robustness of watermark and to keep the quality of embedded image. According to our experimental results, the embedded watermark can successfully survive after attacked by image processing attacks, especially for the JPEG compression. Moreover, since we have employed QIM method for the watermark embedding and extracting processes, our methods are simple and the watermark can be extracted without the original image. Beside, the tradeoff of robustness and quality can be controlled by the parameter Q of QIM and the parameter q of logarithm transform.

Our method requests neither the extra data nor the original image during the extracting procedure. Furthermore, since only the authenticator knows the private key for extraction process, our method can achieve more security.



Figure 13: Some examples of simulation results against common image processing attacks on Lena image with parameters $f_q = 1.2; Q = 0.40g$.

ACKNOWLEDGEMENTS

This work is supported by the Ministry of Education, Science, Sports and Culture, Grant-in-Aid for Scientific Research (A) No.24240001 and (C) No.23500010, a grant of I-System Co. Ltd., NTT Secure Platform Laboratories.

REFERENCES

- F. Y. Shih (eds.), "Digital Watermarking and Steganography: Fundamentals and Techniques," Taylor & Francis Group, CRC Press, Inc., Boca Raton, FL, USA, 2008.
- M. M. Yeung, "Digital watermarking," Commun. ACM, vol. 41, no. 7, 1998.
- A. Nikolaidis, I. Pitas, "Asymptotically optimal detection for additive watermarking in the DCT and DWT domains," IEEE Trans. Image Process., vol. 12, no. 5, pp. 563–571, 2003.
- P. Bao, X. Ma, "Image adaptive watermarking using wavelet domain singular value decomposition," IEEE Trans. Circuits and Systems for Video Technology, vol. 15, no. 1, pp. 96–102, 2005.
- R. Liu, T. Tan, "An SVD-based watermarking scheme for protecting rightful ownership," IEEE Trans. Multimedia, vol. 4, no. 1, pp. 121–128, 2002.
- F. Liu, Y. Liu, "A watermarking algorithm for digital image based on DCT and SVD", Proc. of CISP '08, vol. 1, pp. 380–383, 2008.
- Z. Lu, H. Zheng, J. Huang, "A digital watermarking scheme based on DCT and SVD," Proc. of IHHMSP '07, vol. 1, pp. 241–244, 2007.
- E. Yavuz, Z. Telatar, "SVD adapted DCT domain DC sub-band image watermarking against watermark ambiguity," Proc. of IW-MRCS2006, LNCS, vol. 4105, pp. 66–73, 2006.
- W. Cao, Y. Yan, S. Li, "Robust image watermarking based

- on singular value decomposition in DT-CWT domain," Proc. of IST '09, pp. 381–384, 2009.
- E. Yavuz, Z. Telatar, "Improved SVD-DWT based digital image watermarking against watermark ambiguity," Proc. of SAC '07, pp. 1051–1055, 2007.
- L. Zhang, A. Li, "Robust watermarking scheme based on singular value of decomposition in DWT domain," Proc. of APCIP '09, vol. 2, pp. 19–22, 2009.
- K. Deb, M. Al-Seraj, M. Hoque, M. Sarkar, "Combined DWT-DCT based digital image watermarking technique for copyright protection," Proc. of ICECE '12, pp. 458–461, 2012.
- L. P. Feng, L. B. Zheng, P. Cao, "A DWT-DCT based blind watermarking algorithm for copyright protection," Proc. of ICCSIT, vol. 7, pp. 455–458, 2010.
- Y. Bei, D. Yang, M. Liu, L. Zhu, "A multi-channel watermarking scheme based on HVS and DCT-DWT," Proc. of CSAE '11, vol. 4, pp. 305–308, 2011.
- C. C. Lai, "A digital watermarking scheme based on singular value decomposition and tiny genetic algorithm," Digital Signal Process., no. 21, vol. 4, pp. 522–527, 2011.
- B. Zhou, J. Chen, "A Geometric Distortion Resilient Image Watermarking algorithm Based on SVD," Chinese J. of Image and Graphics, vol. 9, pp. 506–512, 2004.
- G. Bhatnagar, B. Raman, "A new robust reference watermarking scheme based on DWT-SVD", Computer Standards and Interfaces, vol. 31, issue 5, pp. 1002–1013, 2009.
- K. Loukhaoukha, "Comments on "A digital watermarking scheme based on singular value decomposition and tiny genetic algorithm",", Digital Signal Process., vol. 23, issue 4, p. 1334, 2013.
- D. V. S. Chandra, "Digital image watermarking using singular value decomposition," Proc. of the 45th Midwest Symposium on Circuits and Systems (MWSCAS 2002), vol. 3, pp. 264–267, 2002.
- C. C. Chang, P. Tsai, C. C. Lin, "SVD-based digital image watermarking scheme," Pattern Recognition Letters, vol. 26, no. 10, pp. 1577–1586, 2005.
- S. Jia, "A novel blind color images watermarking based on SVD," Optik - International Journal for Light and Electron Optics, vol. 125, issue 12, pp. 2868–2874, 2014.
- C. Tsallis, "Possible generalization of Boltzmann Gibbs statistics," J.Stat. Phys. vol. 52, pp.479–487, 1998.
- T. M. Thanh, P. T. Hiep, T. M. Tam, "A New Spatial q-log Domain for Image Watermarking," International Journal of Intelligent Information Processing (IJIIIP), ISSN 2093-1964, 2014.
- G. Voyatzis and I. Pitas, "Chaotic mixing of digital images and applications to watermarking," European Conf. on Multimedia Applications, Services and Techniques (ECMAST96), vol. 2, pp. 687–695, 1996.
- B. Chen, G. W. Wornell, "Quantization index modulation methods for digital watermarking and information embedding of multimedia," J. VLSI Signal Process. Syst., vol. 27, pp. 7–33, 2001.
- T. M. Thanh, P. T. Hiep, T. M. Tam, K. Tanaka, "Robust semi-blind video watermarking based on frame-patch matching," AEU - International Journal of Electronics and Communications, ISSN 1434-8411, 2014.